PNAS RESEARCH ARTICLE | PHARMACOLOGY OPEN ACCESS

# Serodolin, a β-arrestin–biased ligand of 5-HT$_7$ receptor, attenuates pain-related behaviors

Chayma El Khamlichi[a], Flora Reverchon[a], Nadège Hervouet-Coste[a], Elodie Robin[a], Nicolas Chopin[b], Emmanuel Deau[b], Fahima Madouri[a], Cyril Guimpied[a], Cyril Colas[a,b], Arnaud Menuet[c], Asuka Inoue[d], Andrzej J. Bojarski[e], Gérald Guillaumet[b], Franck Suzenet[b], Eric Reiter[f], and Séverine Morisset-Lopez[a,1]

Edited by Robert Lefkowitz, Howard Hughes Medical Institute, Durham, NC; received October 14, 2021; accepted March 28, 2022

**G protein–coupled receptors (GPCRs) are involved in regulation of manifold physiological processes through coupling to heterotrimeric G proteins upon ligand stimulation. Classical therapeutically active drugs simultaneously initiate several downstream signaling pathways, whereas biased ligands, which stabilize subsets of receptor conformations, elicit more selective signaling. This concept of functional selectivity of a ligand has emerged as an interesting property for the development of new therapeutic molecules. Biased ligands are expected to have superior efficacy and/or reduced side effects by regulating biological functions of GPCRs in a more precise way. In the last decade, 5-HT$_7$ receptor (5-HT$_7$R) has become a promising target for the treatment of neuropsychiatric disorders, sleep and circadian rhythm disorders, and pathological pain. In this study, we showed that Serodolin is unique among a number of agonists and antagonists tested: it behaves as an antagonist/inverse agonist on G$_s$ signaling while inducing ERK activation through a β-arrestin–dependent signaling mechanism that requires c-SRC activation. Moreover, we showed that Serodolin clearly decreases hyperalgesia and pain sensation in response to inflammatory, thermal, and mechanical stimulation. This antinociceptive effect could not be observed in 5-HT$_7$R knockout (KO) mice and was fully blocked by administration of SB269-970, a specific 5-HT$_7$R antagonist, demonstrating the specificity of action of Serodolin. Physiological effects of 5-HT$_7$R stimulation have been classically shown to result from G$_s$-dependent adenylyl cyclase activation. In this study, using a β-arrestin–biased agonist, we provided insight into the molecular mechanism triggered by 5-HT$_7$R and revealed its therapeutic potential in the modulation of pain response.**

analgesia | biased ligands | GPCR | 5-HT7 receptor | serotonin

## Significance

Transmembrane signaling through G protein–coupled receptors (GPCRs), originally described as requiring coupling to intracellular G proteins, also uses G protein–independent pathways through β-arrestin recruitment. Biased ligands, by favoring one of the multiple bioactive conformations of GPCRs, allow selective signaling through either of these pathways. Here, we identified Serodolin as the first β-arrestin–biased agonist of the serotonin 5-HT$_7$ receptor. This new ligand, while acting as an inverse agonist on G$_s$ signaling, selectively induces ERK activation in a β-arrestin–dependent way. Importantly, we report that Serodolin decreases pain intensity caused by thermal, mechanical, or inflammatory stimuli. Our findings suggest that targeting the 5-HT$_7$R with β-arrestin–biased ligand could be a valid alternative strategy to the use of opioids for the relief of pain.

Among 14 serotonin receptor subtypes, 5-hydroxytryptamine 7receptors (5-HT$_7$Rs) belong to the G protein–coupled receptor (GPCR) family or the so-called seven transmembrane-spanning receptor. It is the last identified member and has been cloned from several animal species, including human (1). 5-HT$_7$R couples to the heterotrimeric G protein G$_s$, which in turn stimulates adenylate cyclase (AC), leading to an increase of 3′-5′-cyclic adenosine monophosphate (cAMP) production in both recombinant and native systems (1). This allows the activation of cAMP-dependent protein kinase (PKA), which acts on the MAPK cascade in a cell type–specific manner (2–4).

In HEK-293 cells, the observed agonist-induced ERK1/2 activation requires PKA, Ras, and Raf activation independently of Rap-1 (4). In neurons, the 5-HT$_7$R–induced ERK activation is mediated through a PKA-independent pathway that utilizes cAMP-guanine nucleotide exchange factor (cAMP-GEF) (3). It was shown that 5-HT$_7$R signaling also depends on the activation of Gα$_{12}$ protein that in turn triggers activation of multiple signaling pathways through the family of small Rho GTPases, Cdc42 and RhoA (5).

The 5-HT$_7$R is expressed in the peripheral and central nervous system with highest densities in thalamus, hypothalamus, cerebral cortex, amygdala, and striatal complex (1). Numerous data have established 5-HT$_7$R implication in the control of circadian rhythms and thermoregulation, learning, and memory as well as in central nervous system (CNS) disorders such as depression, Alzheimer's disease, and schizophrenia (6). There is mounting evidence that 5-HT$_7$R is an important modulator of nociceptive transmission (7). It was also reported that 5-HT$_7$R is involved in the antinociceptive effects of morphine (8), antidepressants, and nonopioid analgesics (9). Collectively, these observations underscore the interest of developing new 5-HT$_7$R ligands for the treatment of pain. To date, many 5-HT$_7$R potent agonists (5-CT, E55888, AS-19, and LP-211) and antagonists (SB269-970 and DR4004) against 5-HT$_7$R have been described (10); these are all ligands that commit the receptor to a G protein–dependent pathway, although few 5-HT$_7$R–biased ligands have been described (11, 12).

Author contributions: C.E.K., F.R., F.M., G.G., F.S., E. Reiter, and S.M.-L. designed research; C.E.K., F.R., N.H.-C., E. Robin, F.M., C.G., C.C., A.M., and E. Reiter performed research; N.H.-C., N.C., E.D., A.I., A.J.B., G.G., F.S., and E. Reiter contributed new reagents/analytic tools; C.E.K., F.R., N.H.-C., E. Robin, F.M., E. Reiter, and S.M.-L. analyzed data; and C.E.K., E. Reiter, and S.M.-L. wrote the paper.

The authors declare no competing interest.

This article is a PNAS Direct Submission.



[1]To whom correspondence may be addressed. Email: severine.morisset-lopez@cnrs-orleans.fr.

This article contains supporting information online at http://www.pnas.org/lookup/suppl/doi:10.1073/pnas.2118847119/-/DCSupplemental.

Published May 20, 2022.

In contrast to standard agonists and antagonists, which activate or inactivate the entirety of a receptor's signaling network, some ligands termed biased ligands are capable of stabilizing subsets of receptor conformations, hence eliciting selective modulation within the network. From data obtained in the last two decades, the concept of functional selectivity of a ligand has emerged as an interesting property in modern drug discovery. Increasing preclinical data highlight the value of using such ligands, which exhibit a unique spectrum of pharmacological responses, for instance, by specifically targeting G protein– or β-arrestin–dependent signaling. Biased ligands, by selectively modulating a subset of receptor functions, may optimize therapeutic action and generate less pronounced side effects than compounds globally affecting receptor activity. Although binding of β-arrestins to GPCR has primarily been involved in the termination of G protein signaling by inducing desensitization and internalization of the receptor, numerous studies have indicated that β-arrestins can be intimately involved in additional signaling events through mechanisms dependent on or independent of G protein coupling (13, 14). Several β-arrestin–biased ligands have been identified and show therapeutic interest in other receptor classes (15). In particular, several studies demonstrate the role of β-arrestin signaling on opioid analgesia and tolerance (16, 17). In the present study, we used a combination of pharmacological, genetic, and behavioral approaches to identify a β-arrestin–biased 5-$HT_7$R ligand and evaluate its therapeutical potential for the treatment of pain.

## Results

Though several selective 5-$HT_7$R antagonists have been successfully developed during the past two decades, agonists often suffer from their lack of specificity, inappropriate pharmacokinetic (PK) properties, or their poor ability to cross the blood brain barrier (BBB), precluding their use in clinical development (10). We previously identified a class of potent 5-$HT_7$R antagonists derived from pharmacomodulation studies (18). In this study, we decided to decipher the pharmacological properties of these compounds on various signaling pathways as well as their therapeutic potential.

**Identification of Serodolin, a Biased Ligand with Differential Effects on AC and ERK Pathways.** The HEK-293 cell line stably expressing 5-$HT_7$ receptor was used to compare the effect of different 5-$HT_7$R ligands (Fig. 1*A* and *SI Appendix*, Fig. S1*A*) on the classical $G\alpha_s$-mediated activation of the AC pathway. We decided to evaluate the lead compounds from two series of ligands, Serodolin and MOA-51 (Fig. 1*A*). Both ligands behave as potent antagonists by decreasing the 5-carboxamidotryptamine (5-CT)–induced cAMP accumulation (half maximal inhibitory concentration [$IC_{50}$] = 5 ± 2 nM and 12 ± 6 nM, respectively), similar to the reference antagonist SB269-970 ($IC_{50}$ = 2 ± 1 nM) (Fig. 1*B*). As expected, 5-CT, as well as E55888, two well-described full 5-$HT_7$ receptor agonists, induced a concentration-dependent accumulation of cAMP in HEK-293 cells expressing 5-$HT_7$R (Fig. 1*B* and *SI Appendix*, Fig. S1*B*). In contrast, when tested alone, Serodolin and MOA-51, like SB269-970, produced inverse agonist effects on the cAMP response, inhibiting cAMP production by around 75% with high potency ($IC_{50}$ = 14 ± 6 and 17 ± 6 nM, respectively) (Fig. 1*B*). Interestingly, the dose–response curve of cAMP production induced by increasing doses of 5-CT has a Hill coefficient greater than 1, suggesting a positive cooperativity that could be due to an allosteric interaction with the $G_s$ protein or to homodimerization of the 5-$HT_7$R as previously described (19).

In mock-transfected HEK-293 cells, we did not observe any modification of basal cAMP levels induced by 5-$HT_7$R ligands, consistent with the fact that HEK-293 cells do not express 5-$HT_7$R endogenously (18). Considering previous studies that demonstrated the activation of the ERK pathway downstream of $G_s$ coupling to 5-$HT_7$R (4), we decided to investigate the effect of Serodolin and MOA-51 on ERK response. ERK phosphorylation was monitored by Western blotting after treatment of cells with 10 μM of ligands at different times ranging from 2 to 60 min. As previously described (3, 4), we observed a transient phosphorylation of ERK upon 5-CT exposure (Fig. 1*C*). Cells treated with E55888, another known 5-$HT_7$ agonist, also induce ERK phosphorylation (*SI Appendix*, Fig. S1 *C* and *D*). However, unexpectedly, Serodolin and MOA-51 were found to robustly induce ERK phosphorylation (309 ± 34% and 278 ± 55% of control at the maximal effect) (Fig. 1*C*). Interestingly, when we tested other known 5-$HT_7$R antagonists, such as SB269-970, EGIS-1a (20), or DR4004 (21), none of them were able to induce ERK activation (*SI Appendix*, Fig. S2), underlying the unique pharmacological profile of Serodolin and MOA-51. The kinetics of ERK phosphorylation elicited by 5-CT, E55888, Serodolin, and MOA-51, were very similar: Activation was fast and transient and reached a peak between 2 and 7 min after drug exposure. However, ERK phosphorylation induced by Serodolin and MOA-51 was more protracted compared to 5-CT, the reference agonist. This effect is not due to nonspecific off-target effects, since neither Serodolin nor MOA-51 was able to induce ERK phosphorylation when tested in HEK-293 mock cells (*SI Appendix*, Fig. S3). Considering the more pronounced effect of Serodolin on the ERK pathway compared to MOA-51, we decided to focus our attention on Serodolin for further analyses. Importantly, we demonstrated using immunocytochemistry that Serodolin-induced ERK phosphorylation also occurs in primary neuronal cells endogenously expressing 5-$HT_7$R (Fig. 1*D*) and therefore is not limited to heterologous cellular models overexpressing high levels of receptors. Similar to 5-CT, Serodolin induced a concentration-dependent increase of ERK phosphorylation in HEK-293 cells stably expressing 5-$HT_7$R (Fig. 2 *A* and *B*). Moreover, this effect was fully blocked by coincubation with SB269-970, a selective and highly potent 5-$HT_7$R antagonist (Fig. 2*C*). Collectively, these results revealed that Serodolin displays biased agonism at the 5-$HT_7$R: It behaves as antagonist/inverse agonist of the $G\alpha_s$-AC pathway and as an agonist on ERK phosphorylation.

**Serodolin Induces ERK Phosphorylation through a G Protein–Independent Mechanism.** Because the $G_s$/cAMP/PKA pathway was shown to contribute to ERK phosphorylation by conventional agonist 5-CT, we explored whether this was also the case for a drug with biased efficacy like Serodolin (*SI Appendix*, Fig. S4*A*). In agreement with previous observations, where MAPK activation by 5-CT has been shown to require Ras and MEK activation (4), the 5-CT response on the ERK pathway could not be observed in cells pretreated with FTI277 or PD98059, selective Ras and MEK inhibitors, respectively. Here, we demonstrated that Serodolin-induced ERK phosphorylation is also fully blocked by pretreatment with either of these kinase inhibitors, supporting a role of Ras and MEK in the Serodolin downstream signaling pathway (*SI Appendix*, Fig. S4 *B* and *C*). Several studies have shown that $G_s$-coupled receptors can activate the MAPK cascade through EGFR transactivation (22). However, PD15035, an EGFR kinase inhibitor did not influence the 5-CT

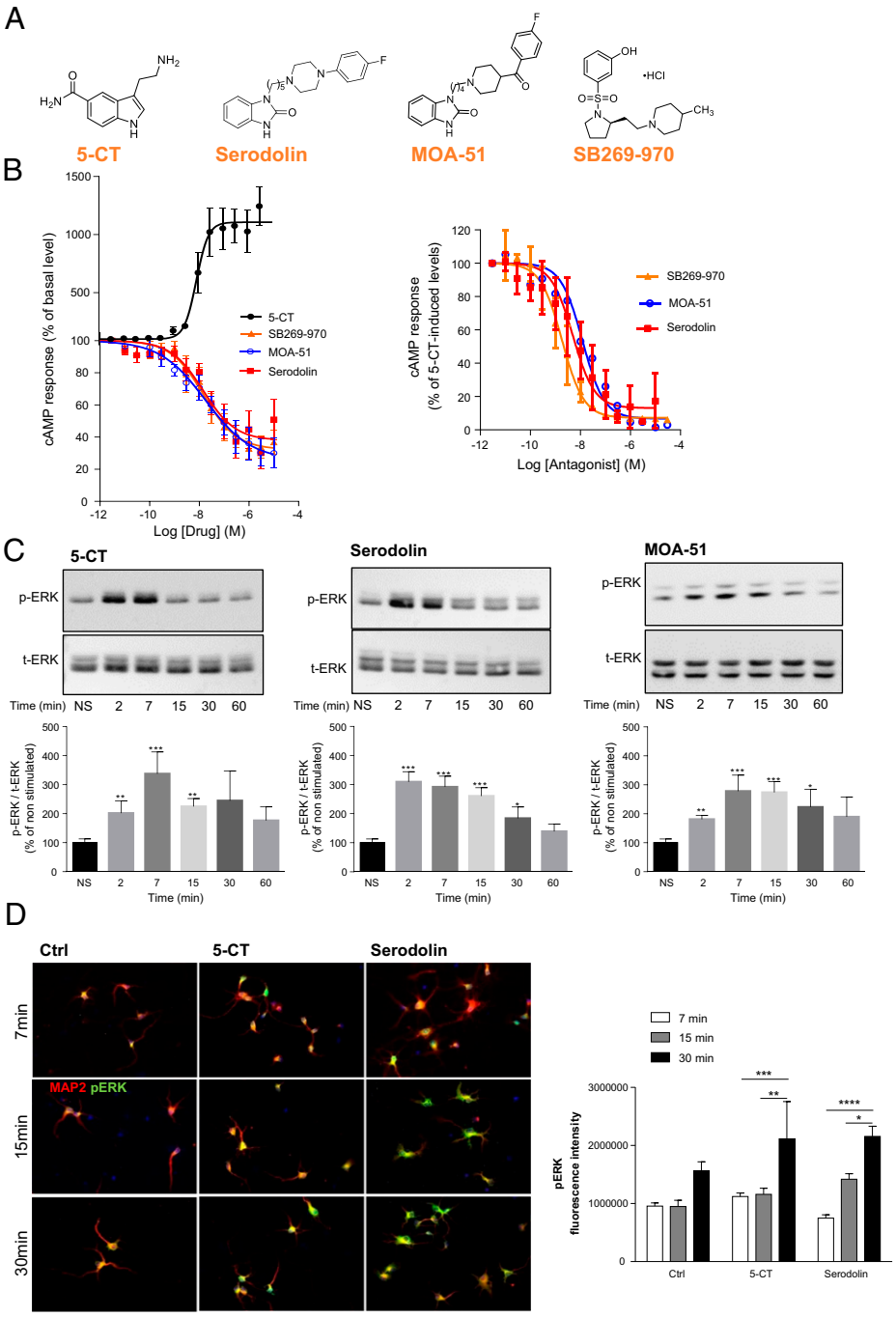


**Fig. 1.** Serodolin and MOA-51 act as antagonists/inverse agonists on $G_s$/cAMP signaling and as agonists on ERK1/2 signaling. (*A*) Chemical structure of 5-$HT_7$R ligands. (*B*) *Left*, HEK-293 cells stably expressing h5-$HT_7$R were incubated with increasing concentration of 5-CT, SB269-970, Serodolin, or MOA-51. (*B*) *Right*, HEK-293 cells stably expressing h5-$HT_7$R were stimulated with 10 nM of 5-CT and increasing concentrations of products for 1 h. After cell lysis, cAMP production was quantified by a LANCE cAMP Detection Kit (Perkin-Elmer). Data points represent the means ± SEM from three independent experiments performed in triplicate. The $EC_{50}$ and $IC_{50}$ for each drug was determined using GraphPad Prism software. (*C*) Time course of activation of ERK1/2 after stimulation of HEK-293 cells stably expressing h5-$HT_7$R with various 5-$HT_7$R ligands used at 10 μM. The cells were stimulated for the indicated periods and assayed for detection of phospho-ERK1/2 by Western blot analysis. All blots were also probes with anti-ERK1/2 antibody to confirm equal loading. Representative blots of three independent experiments are illustrated. The histogram on the *Bottom* of each panel represents the results of densitometric analyses of three independent experiments. Data are means ± SEM. $*P < 0.05$, $**P < 0.01$, $***P < 0.001$ versus nonstimulated cells (NS). (*D*) Mixed neuronal cultures from mice embryos (E15) were stimulated with the 5-$HT_7$R agonist 5-CT (10 μM), Serodolin (10 μM), or vehicle (0.1% DMSO diluted in PBS solution) used as a control group, for 7, 15, and 30 min. Coimmunostaining of neuron marker MAP2 (red) with pERK (green) corresponding to the condition with 30 min of stimulation. These images are representative of two independent experiments. The histogram represents mean ± SEM of fluorescence intensity from two independent experiments of immunofluorescence staining (150 to 200 cells counted per group). $****P < 0.0001$, $***P < 0.001$, $**P < 0.01$, $*P < 0.05$. Statistical analysis was done using Tukey's multiple comparison test.

or Serodolin-induced ERK phosphorylation (*SI Appendix*, Fig. S4*D*). In the case of the stimulation of the $G_s$-coupled receptor, the elevated level of cAMP is known to induce activation of PKA, which in turn triggers ERK phosphorylation through a Ras-dependent mechanism. To examine the role of PKA, cells were preincubated with the PKA inhibitor H89 before the addition of 5-$HT_7$R ligands. The pretreatment of HEK-293 cells with H89 partially decreased ERK phosphorylation induced by 5-CT,

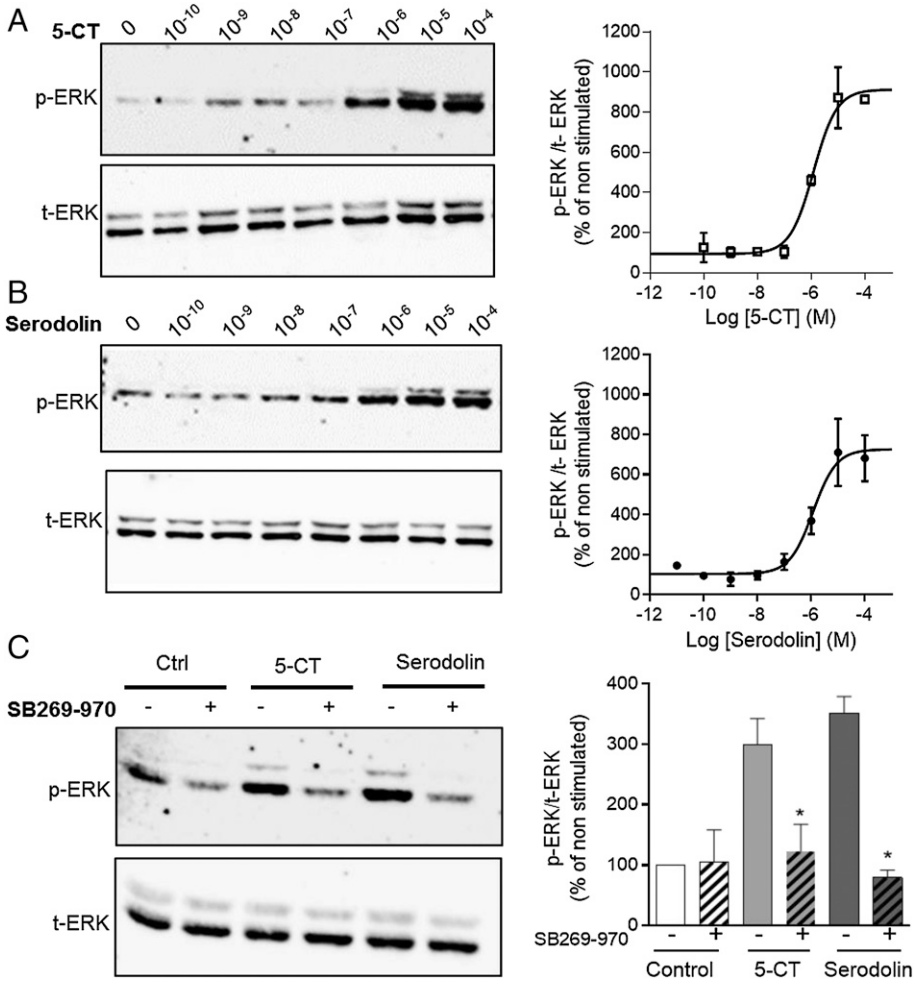


**Fig. 2.** Serodolin-induced ERK phosphorylation is mediated through 5-HT$_7$R activation. (*A* and *B*) HEK-293 cells stably expressing h5-HT$_7$R were stimulated with increasing concentrations of 5-CT or Serodolin for 7 min. (*C*) Cells have been preincubated with SB269-970 (10 μM) for 10 min before the addition of 5-CT (10 μM) or Serodolin (10 μM) to verify the specificity of compounds. Cells were lysed, and Western blot analysis was performed. Representative Western blots from three independent experiments are shown. The graph on the *Right* of each panel represents the results of densitometric analyses of three independent experiments. Data are means ± SEM. *$P < 0.001$ versus cells without SB269-970.

whereas it had no effect on ERK phosphorylation induced by Serodolin (*SI Appendix*, Fig. S4*E*).

In order to explore other mechanisms involved in the biased effect of Serodolin, we considered the ability of some GPCR ligands to elicit "switches" in GPCR coupling from one Gα subtype to another. For that purpose, we evaluated the effect of Serodolin on the recruitment of different G proteins using variants of mini G (mG) proteins (mG$_s$, mG$_i$, mG$_q$, and mG$_{12}$) (23) corresponding to the four families of Gα subunits fused to a fluorescent protein, in bioluminescence resonance energy transfer (BRET) assays. We used the histamine H$_3$ receptor (H$_3$R), adenosine 2B receptor (A$_{2B}$R) or ghrelin receptor (GHSR) as positive controls for Gα$_i$, Gα$_{12}$, and Gα$_q$ recruitment, respectively. In order to assess the impact of kinetics, a critical aspect in the quantification of biased agonism (24), cells were stimulated with increasing concentrations of compounds, and BRET measurement was recorded in real time over 20 min (*SI Appendix*, Fig. S5). Then, the BRET signals obtained were plotted as concentration/response curve using values obtained at the end points (Fig. 3*A*). The reference agonist 5-CT induced recruitment of G$_s$ proteins with a half maximal effective concentration (EC$_{50}$) value (EC$_{50}$ = 1 ± 0.4 nM), in agreement with that observed on cAMP (Fig. 1*B*). As expected, Serodolin as well as SB269-970 behaved as inverse agonist for Gα$_s$ recruitment. Whereas we observed that stimulation of A$_2$R, H$_3$R, and GHSR agonists can induce the recruitment of their cognate G protein, neither classical (5-CT, SB269-970) nor biased (Serodolin) 5-HT$_7$R ligands were able to induce the Gα$_i$, Gα$_{12}$, or Gα$_q$ recruitment. In contrast, Serodolin behaves as an inverse agonist for Gα$_s$ and Gα$_i$ coupling, suggesting that its effect on 5-HT$_7$R–induced ERK activation is mediated through a mechanism independent of G protein coupling. We confirmed that 5-HT$_7$R–stimulated ERK1/2 activity did not depend on the Gα$_q$/IP3/calcium pathway as we did not observe any modification of intracellular calcium after stimulation of 5-HT$_7$R with 5-CT or Serodolin using a calcium-dependent bioluminescence sensor GFP-aequorin assay (*SI Appendix*, Fig. S6*A*). In addition, pretreatment of cells with the Gα$_i$ inhibitor pertussis toxin (PTX) had no effect on 5-HT$_7$R–mediated accumulation of p-ERK1/2 (*SI Appendix*, Fig. S6*B*). Altogether, our data indicate that Serodolin-mediated ERK phosphorylation in HEK-293 cells expressing 5-HT$_7$R does not require the generation of a classical second messenger dependent on Gα$_s$, Gα$_i$, Gα$_{12}$, or Gα$_q$ proteins.

**Serodolin Triggers the Interaction of the c-SRC–β-Arrestin Complex with a Proline-Rich Motif of 5-HT$_7$R Leading to ERK Phosphorylation.** Interestingly, it was shown that some GPCRs can engage ERK1/2 activation through a scaffolding involving the receptor C-terminal part, c-SRC and β-arrestins (25–27). In

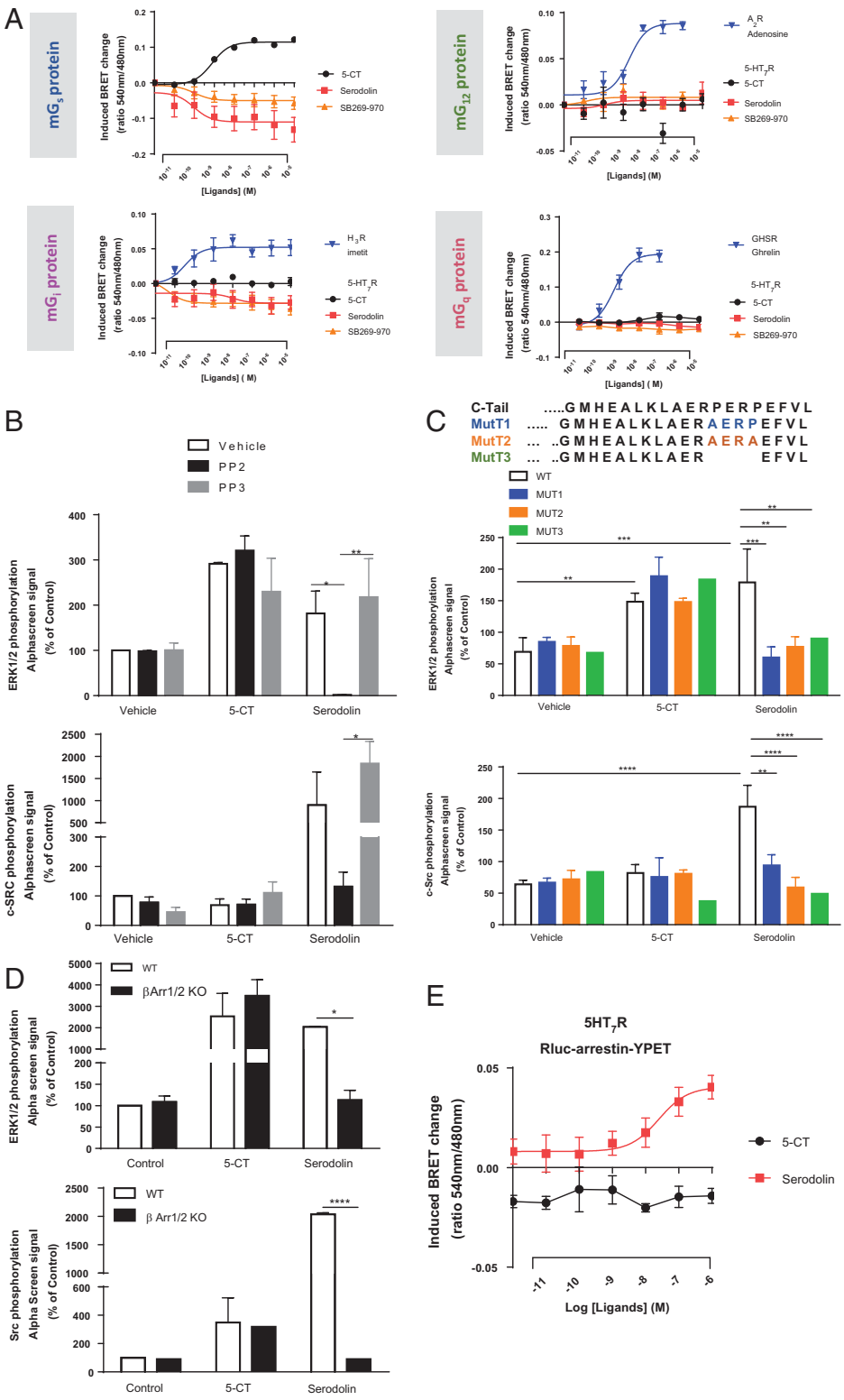


**Fig. 3.** Role of G proteins, c-SRC, and β-arrestin on Serodolin-induced ERK phosphorylation. (*A*) Pharmacological profiling of ligand-mediated G protein recruitment of 5-HT$_7$R receptors using BRET measurement between 5-HT$_7$-RLuc and Venus-mini G proteins. (*B*) Serodolin-induced ERK phosphorylation is dependent on c-SRC activation. HEK-293 cells stably expressing h5-HT$_7$R were stimulated with 5-CT (10 μM) or Serodolin (10 μM) for 7 min in the absence or presence of the potent c-SRC inhibitor PP2 or its inactive analog PP3. Then the effect of 5-CT and Serodolin were evaluated on ERK1/2 and c-SRC activation by Alpha screen assays. (*C*) The PXXP motif in the C-terminal tail of 5-HT$_7$R was mutated as described in the *Upper* panel. The corresponding constructs encoding HA-tagged 5-HT$_7$ receptor were transfected in HEK-293 cells as indicated (mutT1, mutT2, and mutT3), then the effect of 5-CT and Serodolin was evaluated on ERK1/2 and c-SRC activation by Alpha screen assays. (*D*) HEK-293 or KO β-arrestin HEK-293 cells were transiently transfected with HA-5-HT$_7$R and stimulated with 5-CT (10 μM), Serodolin (10 μM), or vehicle (0.1% DMSO diluted in PBS solution) for 7 min, then cell lysates were analyzed by Alpha screen assays. (*E*) HEK-293 cells were transiently transfected with HA-5-HT$_7$R with β-arrestin2 BRET biosensor (Rluc-Arrestin-YPET), then incubated with increasing doses of 5-CT or Serodolin ($10^{-11}$ to $10^{-5}$ M). Ligand-mediated BRET changes are expressed as induced-BRET changes. Data were fitted using nonlinear regression using GraphPad Prism software. Data are means ± SEM. ****$P < 0.0001$, ***$P < 0.001$, **$P < 0.01$, *$P < 0.05$ as indicated.

many cases, β-arrestins function as a scaffold for c-SRC–mediated activation of MAPKs (27–29). Alternatively, c-SRC may be directly activated by binding to GPCR in the absence of β-arrestin (30). To determine whether one of these mechanisms was required for Serodolin-induced ERK phosphorylation, we first evaluated the sensitivity of this activation to the c-SRC–specific tyrosine kinase inhibitor PP2. Importantly, pretreatment with PP2 inhibitor fully blocked the Serodolin-induced ERK phosphorylation, whereas in contrast, it had no effect on ERK phosphorylation induced by 5-CT or E55888 (*SI Appendix*, Fig. S7*A*). PP3, a structural analog of PP2 that does not inhibit c-SRC did not affect 5-$HT_7$R–dependent ERK and c-SRC phosphorylation. In addition, we demonstrated that phosphorylation of c-SRC kinase at Tyr416 was induced only after activation of 5-$HT_7$R by Serodolin and could not be observed after 5-CT or E55888 stimulation (*SI Appendix*, Fig. S7*A*). We confirmed the specific action of Serodolin on c-SRC activation by using the quantitative and highly sensitive AlphaScreen Phospho assays. Using this approach, the Serodolin-induced ERK and c-SRC phosphorylation was fully blocked (by 99% and 100%, respectively) in PP2 pretreatment cells, whereas PP3 was inactive (Fig. 3*B* and *SI Appendix*, Fig. S7*B*). In contrast, the 5-CT– or E5888-induced ERK phosphorylation was not sensitive to PP2 and did not induce c-SRC phosphorylation (Fig. 3*B* and *SI Appendix*, Fig. S7*B*).

Previous studies have shown that proline-rich motifs (PXXP) in the third intracellular loop and the carboxyl terminus of GPCRs are involved in the recruitment of SH3-domain containing proteins (SH3-CPs), like c-SRC (27, 29). Interestingly, we identified such a proline-rich motif in the carboxyl terminus of the 5-$HT_7$R and aimed at dissecting its putative role in c-SRC and ERK activation. To generate proline-deficient 5-$HT_7$R mutants, the proline-rich motif was mutated once or twice with alanine (PXXP AXXP, mut1) and (PXXP AXXA, mut2) or fully deleted (mut3) (Fig. 3*C*, *Upper*). The HA-tagged mutant receptors were well expressed at the plasma membrane and showed cAMP response to 5-CT similar to wild type (WT) (*SI Appendix*, Fig. S8). Interestingly, while all three mutants still responded to 5-CT by inducing ERK phosphorylation, they showed a complete loss of ERK and c-SRC phosphorylation, measured by AlphaScreen assays, upon Serodolin stimulation (Fig. 3*C*). Collectively, these results demonstrate the importance of the PXXP motif of 5-$HT_7$ receptor C terminus in mediating Serodolin-induced signaling.

Previous studies have demonstrated that GPCRs can trigger non-G protein–mediated signaling events and in particular the activation of ERK1/2 by scaffolding complexes composed of c-SRC and β-arrestins. Considering the importance of c-SRC activation in Serodolin-mediated effect, we decided to determine whether β-arrestins are required for Serodolin-stimulated c-SRC–dependent ERK activation. Wild-type HEK-293 cells and β-arrestin–deficient cells generated by using CRISPR-Cas9 gene editing were transfected with HA-5-$HT_7$R (Fig. 3*D*). Serodolin-induced ERK and c-SRC phosphorylation were abolished in β-arrestin knockout (KO) cells, whereas absence of β-arrestins has no effect on 5-CT–induced ERK and SRC responses analyzed by AlphaScreen assays (Fig. 3*D*). A siRNA knockdown approach was then employed to confirm the role of β-arrestins. The siRNA-mediated depletion of β-arrestins completely abrogated Serodolin-stimulated ERK and c-SRC phosphorylation, whereas it did not affect 5-CT–induced ERK phosphorylation (*SI Appendix*, Fig. S9).

We then investigated whether the Serodolin-induced β-arrestin recruitment using an intramolecular fluorescent BRET biosensor RLuc-arrestin-2-YPET (31). Interestingly, in contrast to 5-CT, Serodolin was able to induce a concentration-dependent increase of BRET signal. BRET signal may reflect changes of the conformational states of β-arrestin induced by 5-$HT_7$R activation or may be due to steric interference of the donor and acceptor by recruitment of other binding partners as well as changes in the subcellular environment of the biosensor (Fig. 3*E*). However, corroborating results obtained with silencing β-arrestins, this BRET analysis supports a critical role of β-arrestin in mediating Serodolin signaling.

Altogether, we showed that, in contrast to both reference agonists (E55888 and 5-CT), the Serodolin-induced ERK activation involves c-SRC activation, underlying the specific pharmacological profile of Serodolin. Considering that E55888 is a more selective ligand compared to 5-CT (32), we then used E55888 as a reference agonist for in vivo studies.

**Serodolin Has Antinociceptive Effects in Several Pain Models.** Several studies have suggested that systemic administration of 5-$HT_7$R agonists, such as E55888, resulted in antiallodynic and antihyperalgesic effects in pain conditions involving central sensitization (32). In line with these data, spinal blockade of 5-$HT_7$R has been reported to inhibit the antinociceptive effect of opioids, supporting the idea that 5-$HT_7$R plays an important role in physiological mechanisms controlling nociception and pain (7). Therefore we aimed at evaluating the antinociceptive profile of Serodolin in different types of pain models.

Analgesic activity was first evaluated using the acetic acid abdominal constriction test (writhing test), a chemical model of visceral pain. We evaluated the dose–response effect of Serodolin following single oral, intravenous, and subcutaneous administration of the compound 1 h before injection of acetic acid (Fig. 4*A* and *SI Appendix*, Fig. S10). Pretreatment of the mice with Serodolin produced a dose-dependent decrease of the acetic acid-induced writhing with a significant effect, even at the lower dosage tested, i.e., 0.1 mg/kg subcutaneous (s.c.). Interestingly, we demonstrated that at the highest dosage, Serodolin was able to inhibit by up to 87% the writhing assay response as compared to the full inhibition produced by morphine (3 mg/kg, s.c.), supporting the therapeutic interest of Serodolin.

We then used three other pain models to investigate the mechanisms involved in the antinociceptive actions of Serodolin in comparison with E55888. First, we evaluated the pharmacokinetics profile of both compounds (*SI Appendix*, Fig. S11). We used the liquid chromatography tandem mass spectrometry (UPLC-MS/MS) method to perform a PK study and measure Serodolin versus E55888 levels in vivo. The kinetics demonstrate the presence of both compounds for the same time period during experiments and their ability to pass the brain blood barrier. They show a maximum of detection at 15 to 30 min both in plasma and brain (2.9 ± 0.8 μg/mL for Serodolin and 6.1 ± 0.5 μg/mL for E55888 in plasma and 0.4 ± 0.8 μg/mL for Serodolin and 1.4 ± 0.2 μg/mL for E55888 in brain). However, whereas E55888 is eliminated after 120 min in both plasma and brain, Serodolin is still detected at this time and becomes undetectable after 240 min in plasma and brain.

In the thermal pain model, the mean pooled baseline tail-immersion latency of all the treatment groups was 3.6 ± 0.4 s. Systemic administration of Serodolin (1 and 5 mg/kg, s.c.) produced a significant dose-dependent increase in the tail-immersion latencies (*SI Appendix*, Fig. S12*A*). The effect of Serodolin begun within 10 min postadministration (T0) (*SI Appendix*, Fig. S12*B*) and lasted beyond 70 min (T60) when given in the dose of 5 mg/kg. In comparison with the effect of E55888, Serodolin displayed almost identical behavior on the hot-water immersion tail-flick latencies (Fig. 4*B* and *SI Appendix*, Fig. S12*B*). To

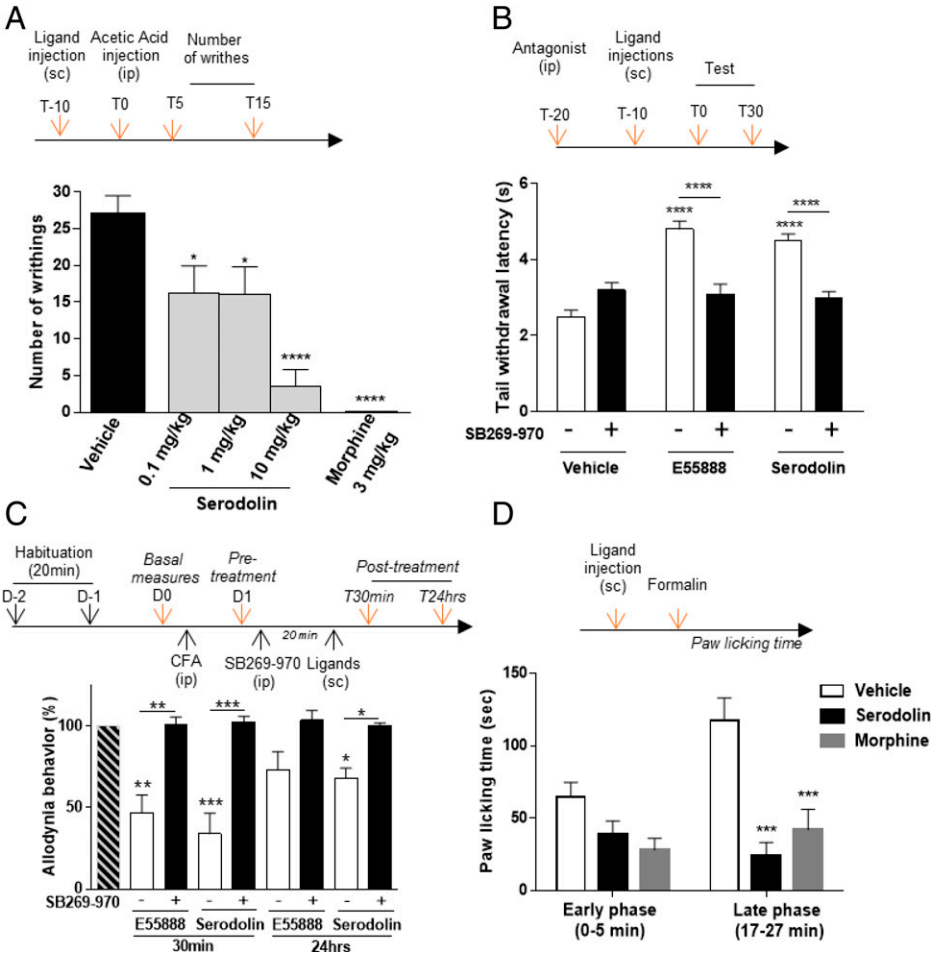


**Fig. 4.** Analgesic and antinociceptive effect of Serodolin. (*A*) Analgesic effect of Serodolin in the acetic acid–induced writhing test. In this test, nociception was induced by an intraperitoneal injection (i.p.) of 0.1 mL/10 g acetic acid solution (10 mL/kg). Serodolin at increasing dosage was administrated by s.c. route before acetic acid injection (*Upper*). Positive control animals were pretreated with morphine (3 mg/kg, s.c.) 10 min before acetic acid. Five minutes after injection of acetic acid, the number of writhing responses was recorded for 10 min. Data are mean ± SEM of values obtained from a representative experiment ($n$ = 10 animals/group). ****$P$ < 0.0001, ***$P$ < 0.001, **$P$ < 0.01, *$P$ < 0.05 as compared with the control group. (*B*) Antinociceptive effect of the 5-HT$_7$R agonist Serodolin on the tail immersion test. Mice were s.c. injected with two 5-HT$_7$ receptor agonists (Serodolin or E55888 at 5 mg/kg) and 10 min later their tail extremity was immersed in water heated to 50 °C. The effect of injections (Serodolin or E55888) was evaluated at T30 corresponding to 40 min after compound injections. ****$P$ < 0,0001 versus vehicle or as indicated. (*C*) Mechanical hypersensitivity was evaluated after CFA intraplantar injection by using the Von Frey test. Mechanical hypersensitivity was performed 30 min after (pretreatment) CFA intraplantar injection into the left hindpaw (ipsilateral paw). Mice were intraperitoneally injected (+) or not (–) with the 5-HT$_7$R antagonist SB269-970, 20 min before agonist subcutaneous injections (E55888 or Serodolin at 5 mg/kg). The ligand effects (E55888 or Serodolin) were evaluated 30 min and 24 h after injection in the ipsilateral paw and reported at 100% allodynia of each mouse. Data are means ± SEM of values obtained in two independent experiments ($n$ = 8 to 10 per group). ****$P$ < 0.0001, ***$P$ < 0.001, **$P$ < 0.01, *$P$ < 0.05. Statistical analysis was done using the Kruskal–Wallis test. (*D*) Effect of the administration of Serodolin (10 mg/kg, s.c.) in the formalin test in rats. Results are expressed as mean ± SEM. Percentages are expressed as decreased as compared to the vehicle-treated group. ***$P$ < 0.001 as compared to the vehicle-treated group; Bonferroni's test after significant two-way repeated measures ANOVA.

validate the specificity of action of both compounds on 5-HT$_7$R, we evaluated whether SB269-970, the selective and potent 5-HT$_7$ antagonist could reverse their antinociceptive properties. While SB269-970 administrated alone did not exert any significant effect on acute thermal nociception, it reversed the analgesia induced by either E55888 or Serodolin at both times tested (Fig. 4*B* and *SI Appendix*, Fig. S12*C*). To reinforce the role played by 5-HT$_7$R in Serodolin-mediating analgesia, we tested its effect in homozygous mice carrying a deletion in the 5-HT$_7$R gene (5-HT$_7$R KO mice). The subcutaneous administration of E55888 and Serodolin did not exert any antinociceptive effect in 5-HT$_7$R KO mice (*SI Appendix*, Fig. S13). These finding clearly establish that systemic administration of Serodolin, a β-arrestin–biased 5-HT$_7$R ligand can generate behavioral antinociception through biased 5-HT$_7$R activation.

We further explored the antinociceptive activity of Serodolin in vivo by evaluating its effect in the control of hypersensitivity following complete Freund's adjuvant (CFA) sensitization. Mice injected with CFA into the midplantar surface of the left hindpaw (ipsilateral paw) developed mechanical hypersensitivity, evidenced by a reduction (>50%) of the mechanical threshold triggering withdrawal of the ipsilateral paw in the Von Frey test, 30 min after injection (Fig. 4*C*). We wanted to evaluate the effect of Serodolin on mechanical hypersensitivity in comparison with E55888 after CFA injection. As expected, subcutaneous administration of E55888 30 min after CFA injection reversed the CFA-induced mechanical hypersensitivity. Significantly decreased paw withdrawal thresholds (antiallodynia) in mice treated with Serodolin were also observed 30 min after administration of 5 mg/kg compared to vehicle-treated mice. Interestingly, when tested 24 h later after administration of 5-HT$_7$R ligands, the antiallodynic effect of Serodolin on CFA-induced hypersensitivity was still significant (Fig. 4*C*). Importantly, pretreatment of animals with SB269-970 30 min before

Serodolin or E55888 administration fully blocked their effect on allodynia (Fig. 4*C*).

Finally, we evaluated the effect of Serodolin in rats in the formalin test, an acute and tonic pain model based on the use of a chemical stimulus. Subcutaneous injection of formalin into the right hindpaw produces a biphasic painful response of increasing and decreasing intensity for about 30 min after the injection. The initial phase of the response (early phase), likely caused by a burst of activity from C fibers, begins immediately after the formalin injection and lasts about 5 min. Although not significant, Serodolin and morphine have an inhibitory effect (−40% and −57%, respectively) during the early phase. Interestingly Serodolin significantly inhibited licking (−80%) and to the same extent as morphine (−64%) during the late phase of formalin-induced behaviors (Fig. 4*D*). These results strongly suggest the potential analgesic effects of Serodolin for states of persistent pain in which tissue damage occurs.

Overall, our results conducted in HEK cells show that serodolin is an antagonist/inverse agonist of G protein signaling, whereas it behaves as an agonist on arrestin signaling. While E55888 and serodolin have opposite effects on the $G_s$ pathway, the first one acting as a full agonist and the second as an inverse agonist, both molecules produce the same effect in three pain models. These results suggest that the arrestin pathway is involved in the effect of Serodolin to alleviate pain-related behaviors.

## Discussion

In the present study, we demonstrated that Serodolin behaves as a 5-$HT_7$R–biased ligand with dual efficacy. Indeed, a detailed pharmacological characterization revealed that Serodolin acts as a potent inverse agonist for $G_s$ signaling while inducing an agonistic response on the ERK pathway. In agreement with previous studies obtained showing stimulation of 5-$HT_7$R with the natural ligand 5-HT (3, 4, 33), we reported that the 5-CT–induced ERK activation requires $G_s$/cAMP/PKA/Ras signaling. In contrast, the Serodolin-induced ERK activation does not requires G protein activation. Rather, Serodolin reduces 5-$HT_7$R basal AC activity and inhibits its constitutive interaction with $G_s$ protein, revealing a robust inverse agonist property. Of particular interest is the finding that other 5-$HT_7$ ligands defined as inverse agonists by their ability to decrease basal AC activity, were not able to induce ERK phosphorylation. Therefore, among 5-$HT_7$R ligands, the pharmacological profile of Serodolin is unique. Our results are in agreement with a multistate model of receptor activation in which ligand-specific conformations are capable of differentially activating distinct signaling partners, as demonstrated initially with the β2 adrenergic receptor (34). In this concept, whereas balanced agonists are able to activate all aspects of GPCR signaling, biased ligands are capable of stabilizing only the subset of conformations, which selectively activate part of the signaling pathway repertoire. For example, ligands can display bias toward either G protein (G protein–biased ligand)– or β-arrestin (β-arrestin–biased ligand)–mediated signaling (15, 35, 36).

Because both G proteins (4) and β-arrestins (33) have been shown to contribute to the 5-$HT_7$R–dependent ERK signaling in response to the natural ligand serotonin, we sought to determine the contribution of each pathways in Serodolin-induced ERK signaling. Consistent with previous studies (3, 4, 33), we demonstrated that stimulation of 5-$HT_7$R by the conventional agonist 5-CT depends on $G_s$/cAMP/PKA signaling as confirmed by the inhibitory effect of H-89 and FTI277, a PKA and a Ras inhibitor, respectively. However, we found no implication of PKA in the Serodolin-induced ERK activation, suggesting a different molecular mechanism for both ligands. As Serodolin is sensitive to β-arrestin knockdown while 5-CT is not, we hypothesized that the 5-$HT_7$R conformation induced by Serodolin might be different from the one induced by 5-CT and allow β-arrestin signaling.

To date, only one compound has been characterized as a β-arrestin–biased ligand at 5-$HT_7$R; however, it displays a submicromolar potency on the $G_s$ pathway and a low efficacy on β-arrestin signaling (11). In addition, whereas some authors reported β-arrestin recruitment upon 5-HT stimulation using the NanoBiT assays (33) or the TANGO reporter system (11), others failed to observe such interaction (37). While our data demonstrated that β-arrestins are required for Serodolin-induced biased signaling at the 5-$HT_7$R, it remains to be determined whether β-arrestin is recruited to the Serodolin-occupied 5-$HT_7$R. It has traditionally been considered that β-arrestin has to interact with GPCR in order to shift into an active conformation, which is capable of recruiting scaffolding proteins such as ERK cascade members (14). However, using different methodologies, such as confocal microscopy or bioluminescence energy transfer, we were unable to detect Serodolin-induced β-arrestin recruitment to 5-$HT_7$R. This lack of effect may be due to the low affinity of the 5-$HT_7$R to β arrestin or a transient and rapid interaction of β-arrestin with the receptor that is undetectable by experimental conditions. If β-arrestin remains in the active conformations after receptor dissociation, this would allow β-arrestin coupling to its effectors at a site distinct from the cellular localization of the receptor, thus mediating distant β-arrestin–mediated signaling as proposed for the β2-AR (38). This hypothesis is consistent with a recent report showing that the ligand-activated GPCR acts catalytically to activate β-arrestin trafficking (39).

The role of G proteins in β-arrestin–mediated ERK activation has recently led to controversy. Some mutants of β2AR or AT1AR receptors, which lost the capacity to couple to G proteins, however, retained the ability to activate ERK1/2, underlying the functional role of β-arrestin1/2 in ERK signaling (40, 41). In contrast, other studies revealed that these two GPCRs do not activate ERK when G proteins were depleted by CRISPR-Cas9 technology. Furthermore, depletion of β-arrestin1/2 has no impact on the agonist-induced ERK activation, implying that β-arrestins are dispensable for the GPCR-driven ERK activation (42, 43). In a more recent study, the role of β-arrestins in overall ERK activation by GPCR operating through a G-dependent or G-independent signaling, even in CRISPR-Cas9 knockout cell lines, was reaffirmed (44). In particular, it was shown that the use of β-arrestin–biased ligands was helpful to avoid misinterpretation associated with the rewiring of signaling networks encountered in these knockout cells. In agreement with these observations, our results underscore the role played by β-arrestin in Serodolin-induced ERK activation, which occurs in the absence of G protein signaling. Interestingly, as the responses of ERK to 5-CT only depend on G protein signaling, we can speculate that G proteins and β-arrestins compete for binding sites on 5-$HT_7$R. Because 5-$HT_7$R is preassociated to G protein (45), this may sterically hinder β-arrestin binding to the receptor. Alternatively, 5-CT and Serodolin, by stabilizing different active conformations, may lead to differential phosphorylations of the receptor hence modifying its "barcodes" that can trigger or not β-arrestin–dependent signaling (13, 46).

Consistent with what we show here, it has been previously demonstrated that pertussis toxin did not affect 5-$HT_7$R–mediated ERK signaling (2, 33). However, additional G protein–dependent

signaling via ERK, cannot be ruled out since it was recently shown that receptors known to be positively coupled to adenylate cyclase by $G\alpha_s$ could activate the ERK pathway by direct coupling between $G\alpha_i$ and β-arrestin (47). Furthermore, the authors specify that this coupling between $G\alpha_i$ and β-arrestin is only partially sensitive to pertussis toxin, suggesting that there are different ways to activate ERK: A G protein–independent pathway and a $G_i$-dependent one (47).

It is known that β-arrestins may function as a scaffold for c-SRC–mediated activation of ERK, as previously demonstrated (29). Alternatively, some GPCRs can interact directly with the tyrosine kinase c-SRC in the absence of β-arrestin (30). In order to explore the role of c-SRC in 5-$HT_7$–mediated signaling, we used pharmacological inhibitors of this tyrosine kinase. We identified c-SRC as a molecule that is actually activated after Serodolin stimulation but is not involved in the 5-CT– and E55888-mediated ERK activation, again demonstrating differences in the molecular events implicated in the effect of both ligands. Furthermore, our results clearly demonstrated a critical role of a proline-rich motif in the 5-$HT_7$R distal C terminus in Serodolin-induced ERK and c-SRC signaling, as mutations or deletion in this motif resulted in complete loss of both c-SRC and ERK activation. These results indicate that the binding of Serodolin to the receptor stabilizes a conformation allowing β-arrestin/c-SRC scaffolding, both required to trigger the ERK pathway. As proposed for others GPCRs (27), the interaction of SH3 domains of c-SRC with the PXXP motif in the 5-$HT_7$R C-tail may appear concomitantly with β-arrestin binding, ensuring reciprocal stabilization of the receptor β-arrestin–c-SRC complex. Alternatively, rearrangement of the proline rich motif in the 5-$HT_7$R C tail in response to Serodolin binding may allow interaction with β-arrestin, thereby promoting conformational changes of β-arrestin allowing the PR regions of β-arrestin to interact with the SH3 domains of c-SRC, as proposed for the β2-AR (29).

Over the last few years, an increasing number of studies demonstrated a role of 5-$HT_7$ receptors in pain modulation (7, 48). Here we provide a convergent set of results indicating that Serodolin is able to reduce many aspects of pain-related behaviors such as mechanical allodynia or thermal hyperalgesia. Remarkably, in a peripheral inflammation murine model induced by hindpaw intraplantar injection of CFA, the antiallodynic effects of Serodolin were as efficient and long-lasting as E55888, a reference agonist compound of 5-$HT_7$R. This long-lasting effect is consistent with the pharmacokinetics of Serodolin, which remains detectable 2 h after its administration both in blood and brain. We demonstrated the specific action of Serodolin at 5-$HT_7$R as its effects were fully blocked by SB269-970, an antagonist of 5-$HT_7$R. These data demonstrated the interests of a biased 5-$HT_7$R ligand in the inhibition of the transmission of pain signal, suggesting that such a signal could be mediated through β-arrestin–dependent and G protein–independent signaling mechanism. Depending on the neural circuits responsible for the analgesic effects, the role of arrestins in the signaling of other receptors may also be involved in the antinociceptive effect of Serodolin. Indeed, the central role of β-arrestins on opioid analgesia and tolerance has already been demonstrated in the case of the mu-opioid receptor (16, 17, 49, 50). If the β-arrestin2 KO mice showed enhanced and prolonged morphine-induced analgesia (17), they also showed a limiting opioid-induced reward (16). Although the role of β-arrestins in 5-$HT_7$R–mediated analgesia should be further investigated, this study revealed the interest of β-arrestin–biased ligands as a therapeutic agent. Corroborating these observations, previous studies have revealed the antinociceptive effect of 5-$HT_7$R activation; administration of 5-$HT_7$R agonists (E57431 and E55888) was found to inhibit the mechanical hypersensitivity secondary to capsaicin injection or nerve injury (32, 51). Spinal 5-$HT_7$R was shown to play a significant inhibitory role in descending serotoninergic modulation in pain induced by inflammation (52) or thermal stimulation (8). Therefore, the Serodolin-induced antinociceptive effects may involve the activation of 5-$HT_7$R at the spinal level and/or in brain areas. Interestingly, it was shown by positron emmision tomography imaging that biased ligands of 5-$HT_{1A}$R can induce differential activation patterns in brain (53). It would be interesting to investigate in future, which brain regions and which neuronal circuits contribute to the therapeutic action of Serodolin.

Interestingly, it has been shown that the capacity of some GPCR-biased ligands to activate specific signaling while blocking or decreasing unwanted actions might have therapeutic benefit (15). As both E55888 and Serodolin induce ERK activation, this suggests a potential role of ERK-mediating signaling in the antinociceptive effects even if other signaling pathways downstream of β-arrestins or G proteins may contribute to the therapeutic effects. The characterization of β-arrestin–biased ligands would help to determine and decipher the respective roles of G protein and β-arrestin signaling in regulation physiological functions mediated by 5-$HT_7$R. Finally, the present findings not only demonstrate the interest of 5-$HT_7$R–biased ligand to reduce pain behavior but also point out the role of β-arrestin signaling in this effect, which opens a potential for therapeutic use of 5-$HT_7$R β-arrestin–biased ligands in the field of analgesia.

## Materials and Methods

**Drugs, Antibodies, Reagents, and Medium.** Coelenterazine was from Interchim. The protease inhibitor mixture was from Roche. PP2, PP3, and PTX were from Calbiochem. Polyvinylidene fluoride (PVDF) membrane and CL-X film were from GE Healthcare. The Pierce SuperSignal West Dura Extended chemiluminescent substrates and medium for cell culture were from Thermo Fisher Scientific. The rabbit anti-mouse (816720) and goat anti-rabbit (656120), IgG horseradish peroxidase (HRP)-linked whole antibodies were from Life Technologies. All other reagents and culture media were from Sigma-Aldrich. The GHSR fused to Renilla luciferase was kindly provided by Jacques Pantel, Institut National de la Santé et de la Recherche Médicale, Unité Mixte de Recherche 1124, Paris, France. The N-terminal 3× HA-tagged human 5-$HT_{7b}$R was obtained from the cDNA Resource Center (http://www.cdna.org).

**Plasmid Constructs.** The human 5-$HT_7$R fused at its C terminus with Renilla Luciferase (5-$HT_7$-RLuc) construct was obtained by *Nhe*I and *Eco*RI sites insertion upstream and downstream, respectively, of the open reading frame (ORF) of the human 5-$HT_7$R in the pRLuc-N1 vector, that we had previously obtained (54). The 5-$HT_7$R–*Nhe*I forward primer 5′-CGACGTGCTAGCGCCACCATGTACCCATACGATGTTC CAGAT-3′ and the 5-HT7R–*Eco*RI reverse primer 5′-CTGAGCGAATTCGTGATGAATCAT GACCTTTTTTTCTACAG-3′ were used for that purpose. The fragments obtained from the *Bam*H1 restriction of the PCR product were ligated into the pRLucN1 vector linearized by digestion with *Nhe*I and *Eco*RI. Mutations in the PXXP motif were performed by site-directed mutagenesis. All sequences obtained were verified by direct DNA sequencing (MWG Eurofins and Cogenics).

**Cell Cultures and Transfections.** HEK-293 cells and HEK-293 cells stably expressing 5-$HT_{7b}$R were grown in Dulbecco's modified Eagle medium (DMEM) supplemented with 10% (vol/vol) dialyzed fetal calf serum (FCS), 100 U/mL penicillin, and 0.1 mg/mL streptomycin. The HEK-293 KO arrestin cell line was mutated in the ARRB1 and the ARRB2 genes, using the CRISPR-Cas9 genome editing technology as described elsewhere (42, 43, 55).

Cerebral cortexes from mice embryos (E15) were collected and mechanically dissociated in 1 mL of Hanks' balanced salt solution (HBSS) ($-Ca^{2+}$) (Sigma) with Hepes (H3375, Sigma). After addition of 1 mL of HBSS ($+Ca^{+2}$) with Hepes and 1 mL of

decomplemented FCS (12133C, Sigma), samples were centrifuged (1,000 rpm, 30 min) to collect cells in 1 mL of neurobasal medium (GIBCO, Thermo Fisher Scientific). Neuronal differentiation was performed in 24-well plates, during 7 d with three medium changes per week.

For BRET experiments cells were transfected with the calcium phosphate precipitation method. For cAMP determinations, cells were transiently transfected with 10 μg of plasmid/100-mm dish with Lipofectamine 2000 (Invitrogen) and Opti-MEM (Gibco), according to manufacturer's recommendations. Experiments were performed 24 h to 48 h after transfection. siRNA were transfected with Lipofectamine 2000 (Invitrogen) in HEK-293 cells.

**cAMP Accumulation and Functional Assays.** cAMP accumulation was measured with a LANCE cAMP Detection Kit (Perkin-Elmer Life Sciences), according to the manufacturer's instructions and as previously described (54). Concentration/response curves were analyzed using Prism 4 software.

**Flow Cytometry.** Cells were transfected with the different mutants of the receptor fused to HA tag and grown until 70% confluence and washed using complete phosphate buffered saline (PBS) (PBS with 1 mM of $CaCl_2$ and 0.5 mM of $MgCl_2$). Cells were then detached and incubated with antihemagglutinin (HA) from Roche Diagnostics for 60 min, followed by an additional incubation with goat anti-rat (FITC) antibody (ab6840) for 60 min. Isotypic controls were done in parallel by incubation with each corresponding immunoglobulin isotype. After washing, stained cells were analyzed by flow cytometry using a BD LSR cytometer (BD Biosciences) and results from 10,000 cells were analyzed by Cell Quest Pro software. Results are presented as the difference in fluorescence relative intensity between the cells labeled with the antibody versus the cells labeled with the corresponding isotype, and by the overlay histograms displaying the isotypic control and the antibody labeling, for one representative experiment out of two.

**SDS-PAGE and Western Blot.** After lysis, samples were resolved by electrophoresis on 10% sodium dodecyl sulfate–polyacrylamide gel electrophoresis (SDS-PAGE), and transferred electrophoretically to PVDF membranes (GE Healthcare Life Sciences). Membranes were washed in Tris-buffered saline (TBS; pH 7.4) containing 0.1% Tween-20 (TBS-T) and blocked with 5% (wt/vol) dry milk TBS-T for 30 min. Blots were probed with anti-arrestin, antiphospho-ERK, or anti-ERK, antiphospho-SRC, anti-SRC, anti-HA, or anti-GFP, or anti-actin antibodies (1:2,000). Horseradish-peroxidase–conjugated goat anti-rabbit, anti-mouse, or anti-rat antibodies (1:33,000) were used as secondary antibodies. Immunoreactive bands were detected using the Dura detection kit. Protein quantification on blots was performed using Quantity One software (Bio-Rad).

**AlphaScreen Assays.** The AlphaScreen SureFire phospho-ERK and phospho-c-SRC assays (PerkinElmer) were used to quantify p-ERK1/2 and p-c-SRC from HEK-293 cell lysates according to the manufacturer's instructions.

**BRET Analyses.** To evaluate $G\alpha_s$, $G\alpha_q$, and $G\alpha_i$ recruitment, cells were transiently transfected with 5-$HT_7$R(b) C terminally fused with donor Rluc (5-$HT_7$R-Rluc) and acceptor NES-Venus. $mG_s$, or NES-Venus-$mG_{sq}$, or NES-Venus-$mG_{si}$ (kindly provided by N. A. Lambert, Augusta University, Augusta, GA) (23) HEK-293 cells were transfected with HA-5$HT_7$(b)-Rluc and the appropriate BRET acceptors, and then incubated with increasing doses of 5-CT, SB269-970, or Serodolin ($10^{-11}$ to $10^{-5}$ M). To evaluate the recruitment of $mG_i$, $mG_{12}$, and $mG_q$, cells were also transfected with a receptor described as positively coupled to the G protein, the adenosine 2 receptor $A_2$R, the histamine 3 receptor $H_3$R, or the ghrelin receptor GHSR and then stimulated with adenosine, imetit, or ghrelin, respectively. For the assessment of β-arrestin2 recruitment, HEK-293 cells were transiently cotransfected with plasmids coding for 5-$HT_7$R-Rluc and for Rluc-β-arrestin2 yPET (kindly provided by M. G. Scott, Cochin Institute, Paris, France). Forty-eight hours after transfection, BRET measurements were immediately performed upon addition of a rising concentration of different ligands and 5 μM of coelenterazine H. Signals were recorded for 30 min in a Mithras LB 940 Multireader (Berthold), which allows the sequential integration of luminescence signals detected with two filter settings (RLuc filter, 485 ± 10 nm; YFP filter, 530 ± 12 nm). Emission signals at 530 nm were divided by emission signals at 485 nm. The results were expressed as induced-BRET change corresponding to the difference between the BRET ratio observed in control conditions (without ligands) and those obtained after addition of 5-$HT_7$R ligands. The results are shown as mean ± SEM from three independent experiments. Data were plotted and analyzed using GraphPad Prism 4 software for Windows (GraphPad Software, Inc.). For normalization the value of all replicates was divided by the mean of the agonist 5-CT–induced maximal responses and multiplied by 100 for any given read out. Concentration/response curves were fitted by nonlinear regression and saturation curves by a hyperbolic one-binding site equation. The method provided estimates for $EC_{50}$ values and corresponding SEM.

**Animals.** C57BL/6 (Janvier) and 5-$HTR_7$ knockout (5-$HT_7R^{-/-}$) mice maintained on a C57BL/6 background (56) as well as Sprague–Dawley rats (specific pathogen free status, Janvier) were used. For experiments, male animals (8 to 14 wk old) were housed in a temperature (20 to 24 °C)- and relative humidity (45 to 65%)–controlled room and acclimated to a bright cycle (12/12 h). Ligands were solubilized in 20% dimethyl sulfoxide (DMSO), 5% Tween 80 diluted in PBS solution for injection in mice. All animal protocols were carried out according to French government animal experiment regulations and approved by animal ethical committees (Comité d'Ethique pour l'Expérimentation Animale Orléans CE03 and Auvergne C2E2A) and accredited by the French Ministry of Education and Research under national authorization Nos. 1195 and 11887. Animals used in this study were treated according to the guidelines of the Committee for Research and Ethical Issue of the International Association for the Study of Pain (1983) and the European guidelines 2010/63/UE.

**Pharmacokinetic Study in Mice.** The pharmacokinetic study was undertaken to evaluate and compare the quantity of Serodolin and E55888 in plasma and brain samples from C57BL/6 mice (Janvier) at several time points. Seven-week-old C57BL/6 mice ($n = 4$ animals per group) received by subcutaneous injection a unique dose (5 mg/kg) of Serodolin or E55888 (U103013S, Achemblock). The control group received vehicle (solution of 20% DMSO and 5% Tween 80 diluted in NaCl). Mice were killed 15, 30, 60, 120, 240, or 480 min after injection. Blank vehicle mouse brain homogenates and plasma were used to established standard curves of Serodolin or E55888. A reference agonist of the 5-$HT_7$R, 5-CT (0458, Tocris), was chosen as an internal standard and diluted at 0.025 mg/kg in acetonitril. Study samples, brain homogenates, and plasma, were prepared for protein precipitation by adding 85 μL of acetonitril + 5-CT to 20 μL of the samples. Liquid chromatography–high resolution mass spectrometry analysis for PK studies were performed on a maXis quadrupole time-of-flight mass spectrometer (Bruker) coupled to an U3000 rapid separation liquid chromotagraphy ultra-high–performance liquid chromatography system (Dionex). Separation was obtained using an Acquity UPLC BEH C18 column (2.1 × 50 mm; 1.7 μm) (Waters) thermostated at 40 °C with a gradient of water (solvent A) and acetonitrile (solvent B), both acidified with 0.1% formic acid at 500 μL/min. The gradient was as follows: 2% B from 0 to 0.1 min, a linear gradient up to 98% B at 2.4 min, kept to 3.5 min and reconditioning of the column at 2% B from 3.6 to 5.8 min. The samples were randomized prior to the analysis; 1.25 μL was injected into plasma and 8 μL into brains. Mass spectra were recorded in the 50 to 1,650 *m/z* range at a frequency of 4 Hz with positive electrospray ionization. Areas were integrated from extracted ion chromatograms (EIC) of [M+H]+ ions using QuantAnalysis 4.4 software (Bruker) with a tolerance of ± 0.005 unit.

**Immunocytochemistry.** Primary neuronal cells were fixed with 4% paraformaldehyde in PBS for 10 min and then washed with PBS. Cells were saturated with 0.3% Triton X-100 in 1% bovine serum albumin (BSA) in TBS-FCS 10% for 15 min, followed by three washes in TBS and incubated 2 h with rabbit anti-p-ERK (9101 1/200, Cell Signaling) and mouse anti-MAP2 (119942 1/250, Sigma) in TBS with 1% BSA, 10% FCS, and 0.3% Triton X-100. Then, cells were washed three times with TBS and incubated with the corresponding secondary antibodies, sheep anti-rabbit IgG FITC (F7512 1/500, Sigma) or goat anti-mouse IgG TRITC (T7657 1/100, Sigma) for 1 h in a wet and dark room. After three washes, cells were stained with bisBenzimide H33258 (B1155, Sigma) for 10 min and washed and mounted onto microscope slides with Fluoromount-G (0100-01, Southern Biotech). The costainings were observed using an inverted Zeiss Cell Observer 27 microscope with a 40× EC Plan Neofluar 40/0.75 numerical aperture objective (Carl Zeiss Co.). Images were processed with Zen software analyzed with ImageJ.

**Nociception Assessments.**

***Writhing tests.*** Groups of mice ($n = 10$; 25 to 35 g) received Serodolin by oral, subcutaneous, or intravenous route at different doses (0.1 to 10 mg/kg) 1 h before intraperitoneal injection of 1% acetic acid in a volume of 10 mL/kg.

The control group received vehicle (10 mL/kg, solution of 20% DMSO and 5% Tween 80). The test was carried out 5 min later after acetic acid injection. The characteristic writhing responses have been observed individually and counted for 10 min. Measurements were performed by CERB.

***Von Frey filament test.*** Before inducing inflammatory pain, each animal was tested on the left hindpaw with Von Frey filament to determine its basal sensibility level. Then, peripheral inflammation was induced by intraplantar injection of complete Freund's adjuvant (CFA-10 μL) (F5881, Sigma) in the left hindpaw (ipsilateral paw) and mechanical allodynia was measure (pretreatment). Mice were divided into two groups, one with E55888 (5 mg/kg) and the other with Serodolin (5 mg/kg) subcutaneous injections in the ipsilateral paw, treated with (+) or without (-) the 5-$HT_7$R antagonist SB269-960 (5 mg/kg), intraperitoneally injected 20 min before the agonist injections (8 to 10 mice per group). The ligand effects on mechanical allodynia were analyzed 30 min and 24 h after (posttreatment), and the results were reported at 100% of mechanical paw withdrawal threshold of each mouse.

***Tail immersion test.*** Nociception was assessed with the tail immersion test, 10 min and 40 min after E55888 (5 mg/kg) or Serodolin (5 mg/kg) tail subcutaneous injections, in water heated to 50 ± 2 °C. Vehicle (20% DMSO, 5% Tween 80 diluted in PBS solution) was used as a control group. These different groups were intraperitoneally injected (+) or not (−) with the 5-$HT_7$R antagonist SB269-960 (5 mg/kg).

***Formalin test.*** Unilateral injection of a 2.5% formalin solution (50 μL) was performed into the plantar aspect of the hindpaw on testing day. Vehicle, Serodolin (10 mg/kg, s.c.), or morphine (4 mg/kg, s.c.) was adminstered 30 min before a 2.5% formalin solution (50 μL) into the plantar aspect of the hindpaw of rats. Hindpaw licking time was recorded in consecutive 5-min periods from 0 to 5 min (early phase) and 17 to 27 min (late phase) after formalin injection.

**Statistical Analysis.** All results are shown as mean ± SEM. For in vivo experiments, statistical analysis was performed using the nonparametric Kruskal–Wallis test followed by Dunn's posttest or a two-way ANOVA with Tukey's post hoc test. The quantification of p-ERK fluorescence intensity on neuronal culture was analyzed using a two-way ANOVA with Tukey's post hoc test.

**Data Availability.** All study data are included in the article and/or supporting information.

**ACKNOWLEDGMENTS.** We thank Francesco De Pascali for technical assistance. We also thank Catherine Grillon, Martine Decoville, and Pascale Crépieux for helpful discussions and Stéphane Charpentier for fruitful discussions and proofreading of the manuscript. This work was supported by the Region Centre Val de Loire (projects Serosero7 and PAIN), the Structure Fédérative de Recherche (SFR) FED 4226 "Neuroimagerie Fonctionnelle", the Fédération de Recherche Physique et Chimie du vivant FR2708 Centre de Biophysique Moléculaire - Institut de Chimie Organique et Analytique and the University of Orléans. C.E.K. was the recipient of a PhD fellowship from the Region Centre Val de Loire. F.R. was the recipient of a postdoctoral fellowship from the Fondation pour la Recherche Médicale. E.R. is supported by the French National Research Agency under the program "Investissements d'avenir" Grant Agreement LabEx MabImprove: ANR-10-LABX-53 and by "ARD CVL Biomédicaments." E.D., N.C., G.G., and F.S. also acknowledge the projects CHemBio (FEDER-FSE 2014-2020-EX003677), Techsab (FEDER-FSE 2014-2020-EX011313), the Reseau Thématique de Recherche RTR Motivhealth (2019-00131403), and the Labex programs SYNORG (ANR-11-LABX-0029) and IRON (ANR-11-LABX-0018-01) for financial support. A.I. was funded by the Japan Society for the Promotion of Science KAKENHI grants 21H04791 and 21H05113; the Moonshot Research and Development Program JPMJMS2023; the FOREST JPMJFR215T from the Japan Science and Technology Agency; the PRIME JP19gm5910013, the LEAP JP20gm0010004, and the BINDS JP20am0101095 from the Japan Agency for Medical Research and Development; the Daiichi Sankyo Foundation of Life Science and the Uehara Memorial Foundation.

Author affiliations: [a]Centre de Biophysique Moléculaire, CNRS, Unité Propre de Recherche 4301, Université d'Orléans, Orléans Cedex 2, 45071 France; [b]Institut de Chimie Organique et Analytique, Université d'Orléans, CNRS, Unité Mixte de Recherche 7311, Orléans 45067, France; [c]Laboratoire d'Immunologie et Neurogénétique Expérimentales et Moléculaires, CNRS, Unité Mixte de Recherche 7355, Université d'Orléans, Orléans Cedex 2, 45071 France; [d]Graduate School of Pharmaceutical Sciences, Tohoku University, Sendai 980-8578, Japan; [e]Maj Institute of Pharmacology, Polish Academy of Sciences, Kraków 31-343, Poland; and [f]Physiologie de la Reproduction et des Comportements (PRC), Institut National de Recherche pour l'Agriculture, l'Alimentation et l'Environnement (INRAE), Centre National de la Recherche Scientifique (CNRS), Institut Français du Cheval et de l'Equitation (IFCE), Nouzilly 37380, France

1. N. M. Barnes *et al.*, International Union of Basic and Clinical Pharmacology. CX. Classification of receptors for 5-hydroxytryptamine; pharmacology and function. *Pharmacol. Rev.* **73**, 310–520 (2021).
2. M. Errico, R. A. Crozier, M. R. Plummer, D. S. Cowen, 5-HT(7) receptors activate the mitogen activated protein kinase extracellular signal related kinase in cultured rat hippocampal neurons. *Neuroscience* **102**, 361–367 (2001).
3. S. L. Lin, N. N. Johnson-Farley, D. R. Lubinsky, D. S. Cowen, Coupling of neuronal 5-HT7 receptors to activation of extracellular-regulated kinase through a protein kinase A-independent pathway that can utilize Epac. *J. Neurochem.* **87**, 1076–1085 (2003).
4. J. H. Norum, K. Hart, F. O. Levy, Ras-dependent ERK activation by the human G(s)-coupled serotonin receptors 5-HT4(b) and 5-HT7(a). *J. Biol. Chem.* **278**, 3098–3104 (2003).
5. E. Kvachnina *et al.*, 5-HT7 receptor is coupled to G alpha subunits of heterotrimeric G12-protein to regulate gene transcription and neuronal morphology. *J. Neurosci.* **25**, 7821–7830 (2005).
6. K. M. Blattner, D. J. Canney, D. A. Pippin, B. E. Blass, Pharmacology and therapeutic potential of the 5-$HT_7$ receptor. *ACS Chem. Neurosci.* **10**, 89–119 (2019).
7. F. Viguier, B. Michot, M. Hamon, S. Bourgoin, Multiple roles of serotonin in pain control mechanisms–Implications of 5-$HT_7$ and other 5-HT receptor types. *Eur. J. Pharmacol.* **716**, 8–16 (2013).
8. A. Dogrul, M. Seyrek, Systemic morphine produce antinociception mediated by spinal 5-HT7, but not 5-HT1A and 5-HT2 receptors in the spinal cord. *Br. J. Pharmacol.* **149**, 498–505 (2006).
9. L. J. Dam, L. Hai, Y. M. Ha, Role of the 5-HT(7) receptor in the effects of intrathecal nefopam in neuropathic pain in rats. *Neurosci. Lett.* **566**, 50–54 (2014).
10. M. N. Modica *et al.*, Structure-activity relationships and therapeutic potentials of 5-$HT_7$ receptor ligands: An update. *J. Med. Chem.* **61**, 8475–8503 (2018).
11. Y. Kim *et al.*, Discovery of β-arrestin biased ligands of 5-$HT_7$R. *J. Med. Chem.* **61**, 7218–7233 (2018).
12. J. Lee *et al.*, Discovery of G protein-biased ligands against 5-$HT_7$R. *J. Med. Chem.* **64**, 7453–7467 (2021).
13. E. Reiter, S. Ahn, A. K. Shukla, R. J. Lefkowitz, Molecular mechanism of β-arrestin-biased agonism at seven-transmembrane receptors. *Annu. Rev. Pharmacol. Toxicol.* **52**, 179–197 (2012).
14. L. M. Luttrell, R. J. Lefkowitz, The role of beta-arrestins in the termination and transduction of G-protein-coupled receptor signals. *J. Cell Sci.* **115**, 455–465 (2002).
15. E. J. Whalen, S. Rajagopal, R. J. Lefkowitz, Therapeutic potential of β-arrestin- and G protein-biased agonists. *Trends Mol. Med.* **17**, 126–139 (2011).
16. L. M. Bohn *et al.*, Enhanced rewarding properties of morphine, but not cocaine, in beta(arrestin)-2 knock-out mice. *J. Neurosci.* **23**, 10265–10273 (2003).
17. L. M. Bohn *et al.*, Enhanced morphine analgesia in mice lacking beta-arrestin 2. *Science* **286**, 2495–2498 (1999).
18. E. Deau *et al.*, Rational design, pharmacomodulation, and synthesis of dual 5-hydroxytryptamine 7 (5-HT7)/5-hydroxytryptamine 2A (5-HT2A) receptor antagonists and evaluation by [(18)F]-PET imaging in a primate brain. *J. Med. Chem.* **58**, 8066–8096 (2015).
19. M. Teitler, N. Toohey, J. A. Knight, M. T. Klein, C. Smith, Clozapine and other competitive antagonists reactivate risperidone-inactivated h5-HT7 receptors: Radioligand binding and functional evidence for GPCR homodimer protomer interactions. *Psychopharmacology (Berl.)* **212**, 687–697 (2010).
20. B. Volk *et al.*, (Phenylpiperazinyl-butyl)oxindoles as selective 5-HT7 receptor antagonists. *J. Med. Chem.* **51**, 2522–2532 (2008).
21. C. Kikuchi *et al.*, 2a-[4-(Tetrahydropyridoindol-2-yl)butyl]tetrahydrobenzindole derivatives: New selective antagonists of the 5-hydroxytryptamine7 receptor. *J. Med. Chem.* **45**, 2197–2206 (2002).
22. L. A. Grisanti, S. Guo, D. G. Tilley, Cardiac GPCR-mediated EGFR transactivation: Impact and therapeutic implications. *J. Cardiovasc. Pharmacol.* **70**, 3–9 (2017).
23. Q. Wan *et al.*, Mini G protein probes for active G protein-coupled receptors (GPCRs) in live cells. *J. Biol. Chem.* **293**, 7466–7473 (2018).
24. C. Klein Herenbrink *et al.*, The role of kinetic context in apparent biased agonism at GPCRs. *Nat. Commun.* **7**, 10842 (2016).
25. G. Barthet *et al.*, 5-hydroxytryptamine 4 receptor activation of the extracellular signal-regulated kinase pathway depends on Src activation but not on G protein or beta-arrestin signaling. *Mol. Biol. Cell* **18**, 1979–1991 (2007).
26. S. Perkovska *et al.*, $V_{1b}$ vasopressin receptor trafficking and signaling: Role of arrestins, G proteins and Src kinase. *Traffic* **19**, 58–82 (2018).
27. A. Rey, D. Manen, R. Rizzoli, J. Caverzasio, S. L. Ferrari, Proline-rich motifs in the parathyroid hormone (PTH)/PTH-related protein receptor C terminus mediate scaffolding of c-Src with beta-arrestin2 for ERK1/2 activation. *J. Biol. Chem.* **281**, 38181–38188 (2006).
28. K. A. DeFea *et al.*, The proliferative and antiapoptotic effects of substance P are facilitated by formation of a beta -arrestin-dependent scaffolding complex. *Proc. Natl. Acad. Sci. U.S.A.* **97**, 11086–11091 (2000).
29. F. Yang *et al.*, Allosteric mechanisms underlie GPCR signaling to SH3-domain proteins through arrestin. *Nat. Chem. Biol.* **14**, 876–886 (2018).
30. W. Cao *et al.*, Direct binding of activated c-Src to the beta 3-adrenergic receptor is required for MAP kinase activation. *J. Biol. Chem.* **275**, 38131–38134 (2000).
31. P. G. Charest, S. Terrillon, M. Bouvier, Monitoring agonist-promoted conformational changes of beta-arrestin in living cells by intramolecular BRET. *EMBO Rep.* **6**, 334–340 (2005).
32. A. Brenchat *et al.*, 5-HT7 receptor activation inhibits mechanical hypersensitivity secondary to capsaicin sensitization in mice. *Pain* **141**, 239–247 (2009).
33. P. Liu *et al.*, Ligand-induced activation of ERK1/2 signaling by constitutively active $G_s$-coupled 5-HT receptors. *Acta Pharmacol. Sin.* **40**, 1157–1167 (2019).
34. A. W. Kahsai *et al.*, Multiple ligand-specific conformations of the β2-adrenergic receptor. *Nat. Chem. Biol.* **7**, 692–700 (2011).
35. V. V. Gurevich, E. V. Gurevich, Biased GPCR signaling: Possible mechanisms and inherent limitations. *Pharmacol. Ther.* **211**, 107540 (2020).
36. J. W. Wisler, K. Xiao, A. R. Thomsen, R. J. Lefkowitz, Recent developments in biased agonism. *Curr. Opin. Cell Biol.* **27**, 18–24 (2014).

37. K. W. Andressen *et al.*, The atypical antipsychotics clozapine and olanzapine promote down-regulation and display functional selectivity at human 5-HT7 receptors. *Br. J. Pharmacol.* **172**, 3846–3860 (2015).
38. S. Nuber *et al.*, β-Arrestin biosensors reveal a rapid, receptor-dependent activation/deactivation cycle. *Nature* **531**, 661–664 (2016).
39. K. Eichel *et al.*, Catalytic activation of β-arrestin by GPCRs. *Nature* **557**, 381–386 (2018).
40. Z. Gáborik *et al.*, The role of a conserved region of the second intracellular loop in AT1 angiotensin receptor activation and signaling. *Endocrinology* **144**, 2220–2228 (2003).
41. S. K. Shenoy *et al.*, beta-arrestin-dependent, G protein-independent ERK1/2 activation by the beta2 adrenergic receptor. *J. Biol. Chem.* **281**, 1261–1273 (2006).
42. M. Grundmann *et al.*, Lack of beta-arrestin signaling in the absence of active G proteins. *Nat. Commun.* **9**, 341 (2018).
43. M. O'Hayre *et al.*, Genetic evidence that β-arrestins are dispensable for the initiation of $\beta_2$-adrenergic receptor signaling to ERK. *Sci. Signal.* **10**, eaal3395 (2017).
44. L. M. Luttrell *et al.*, Manifold roles of β-arrestins in GPCR signaling elucidated with siRNA and CRISPR/Cas9. *Sci. Signal.* **11**, eaat7650 (2018).
45. K. W. Andressen *et al.*, Related GPCRs couple differently to $G_s$: Preassociation between G protein and 5-$HT_7$ serotonin receptor reveals movement of $G\alpha_s$ upon receptor activation. *FASEB J.* **32**, 1059–1069 (2018).
46. X. E. Zhou *et al.*, Identification of phosphorylation codes for arrestin recruitment by G protein-coupled receptors. *Cell* **170**, 457–469.e13 (2017).
47. J. S. Smith *et al.*, Noncanonical scaffolding of $G_{\alpha i}$ and β-arrestin by G protein-coupled receptors. *Science* **371**, eaay1833 (2021).
48. Q. Q. Liu *et al.*, Role of 5-HT receptors in neuropathic pain: Potential therapeutic implications. *Pharmacol. Res.* **159**, 104949 (2020).
49. Y. Li *et al.*, Improvement of morphine-mediated analgesia by inhibition of β-arrestin2 expression in mice periaqueductal gray matter. *Int. J. Mol. Sci.* **10**, 954–963 (2009).
50. B. Przewlocka *et al.*, Knockdown of spinal opioid receptors by antisense targeting beta-arrestin reduces morphine tolerance and allodynia in rat. *Neurosci. Lett.* **325**, 107–110 (2002).
51. F. Viguier *et al.*, GABA, but not opioids, mediates the anti-hyperalgesic effects of 5-HT7 receptor activation in rats suffering from neuropathic pain. *Neuropharmacology* **63**, 1093–1106 (2012).
52. J. Yang *et al.*, Different role of spinal 5-HT(hydroxytryptamine)7 receptors and descending serotonergic modulation in inflammatory pain induced in formalin and carrageenan rat models. *Br. J. Anaesth.* **113**, 138–147 (2014).
53. B. Vidal *et al.*, In vivo biased agonism at 5-$HT_{1A}$ receptors: Characterisation by simultaneous PET/MR imaging. *Neuropsychopharmacology* **43**, 2310–2319 (2018).
54. W. Deraredj Nadim *et al.*, Physical interaction between neurofibromin and serotonin 5-HT6 receptor promotes receptor constitutive activity. *Proc. Natl. Acad. Sci. U.S.A.* **113**, 12310–12315 (2016).
55. W. Stallaert *et al.*, Purinergic receptor transactivation by the $\beta_2$-adrenergic receptor increases intracellular $Ca^{2+}$ in nonexcitable cells. *Mol. Pharmacol.* **91**, 533–544 (2017).
56. P. B. Hedlund *et al.*, No hypothermic response to serotonin in 5-HT7 receptor knockout mice. *Proc. Natl. Acad. Sci. U.S.A.* **100**, 1375–1380 (2003).